



Machine vision for the maturity classification of oil palm fresh fruit bunches based on color and texture features

Anindita Septiarini^{a,*}, Andi Sunyoto^b, Hamdani Hamdani^a, Anita Ahmad Kasim^c, Fitri Utaminingrum^d, Heliza Rahmania Hatta^a

^a Department of Informatics, Faculty of Engineering, Mulawarman University, Samarinda, Indonesia

^b Faculty of Computer Science, Universitas Amikom, Yogyakarta, Indonesia

^c Department of Information Technology, Faculty of Engineering, Universitas Tadulako, Palu, Indonesia

^d Computer Vision Research Group, Faculty of Computer Science, Brawijaya University, Malang, Indonesia

ARTICLE INFO

Key words:

fruit classification
elaeis guineensis
 features extraction
 principal component analysis
 ANN

ABSTRACT

The quality of oil palm fresh fruit bunch (FFB) specified from the maturity level is visually classified based on the skin colour of the fruit. The maturity level classification of FFB can be performed automatically using machine vision. Classification becomes challenging when machine vision is applied to half-ripe FFB images, which generally have uneven colour, and to FFB images where emergent noise partially covers the fruit. In this work, a method is proposed to classify the maturity level of FFB into three classes: raw, ripe, and half-ripe. The proposed method applied colour and texture features required in the processes of feature selection and classification. The process of feature extraction was applied based on the colour and texture followed by feature selection using principal component analysis (PCA) to select the most substantial features. Subsequently, an artificial neural network (ANN) with a back-propagation algorithm was applied in the classification process to obtain the prediction class. The experiment was conducted using a local dataset consisting of 240 images (80 raw, 80 ripe, and 80 half-ripe). The results showed that the performance of the proposed method successfully achieved an accuracy of 98.3%. This classification based on colour and texture features is not restricted only to palm oil but can also be applied to other fruits.

1. Introduction

Oil palm (*Elaeis guineensis*) is an important agricultural plant globally because it can be used to produce vegetable oil. This plant has to be planted on suitable land to grow well and not harm the surrounding environment (Hamdani et al., 2016). It has become the basic material used to produce several types of products, including food products, such as instant noodles, butter, jam, bread, and cake, and non-food products, such as washing powders, shampoo, soap, and biodiesel (Taparugssanagorn et al., 2015). Therefore, the demand for high-quality palm oil is continuously increasing. The quality of oil palm is determined by the maturity level of the harvested fruit. The maturity levels of oil palm FFB are visually determined based on the skin colour of the fruit. Raw oil palm fruit has a dark colour (dark purple) and gradually turns orange when it ripens. Technology to detect the maturity of oil palm FFB has been developed using various tools, such as image-based laser systems (Ali et al., 2020; Shiddiq et al., 2017), Kinect cameras (Pamornnak et al.,

2017), smartphones (Sinambela et al., 2020; Taparugssanagorn et al., 2015), and other sensor devices (Hafiz et al., 2012; Mohammed et al., 2012).

To date, the field of agriculture has implemented machine vision-based technology to complete several tasks. These tasks include monitoring plant growth (Fahmi et al., 2018; Pérez-Zavala et al., 2018), identifying crop diseases that occur in stems (Khaled et al., 2018) and leaves (Aji et al., 2013; Darwish et al., 2020), segmenting fruit (Pérez-Zavala et al., 2018; Septiarini et al., 2020) and estimating the volume and mass of fruits and vegetables (Jana et al., 2020). In addition, machine vision techniques have also been developed to classify the maturity of several types of fruit (Munera et al., 2019; Piedad et al., 2018; Tan et al., 2018) and vegetables (Ji et al., 2019; Palacios-Morillo et al., 2016). There are two main processes involved in performing maturity classification, namely, feature extraction and classification.

Feature extraction in this application is divided into three types: colour, texture, and shape (Hameed et al., 2018). The types of features

* Corresponding author.

E-mail address: anindita@unmul.ac.id (A. Septiarini).

<https://doi.org/10.1016/j.scienta.2021.110245>

Received 5 October 2020; Received in revised form 25 April 2021; Accepted 28 April 2021

Available online 15 May 2021

0304-4238/© 2021 Elsevier B.V. All rights reserved.



Fig. 1. Examples of FFB images with various levels of maturity: (a) raw, (b) ripe, and (c) half-ripe.

used depend on the variety of fruit. Colour provides valuable information to classify the level of maturity and quality of fruit. Therefore, both of these characteristics in several fruits are determined based on the peel colour. There are several colour spaces commonly used to detect fruit maturity, i.e., red, green, blue (RGB), hue, saturation, intensity (HSI), luminance, in-phase, quadrature-phase (YIQ), blue-difference chroma, red-difference chroma (YCbCr), and $L^*a^*b^*$. RGB is applied to detect the maturity of various fruits, such as dates (Zhang et al., 2014), bananas (Piedad et al., 2018), passion fruits (Tu et al., 2018), and oil palm (Fadilah et al., 2012; Ali et al., 2020; Taparugssanagorn et al., 2015). Furthermore, HSI is applied to blueberries (Li et al., 2014), mangoes (Mim et al., 2018), and oil palm (Makky and Soni, 2013; Shabdin et al., 2016). In contrast, $L^*a^*b^*$ is implemented on bananas (Sanaeifar et al., 2016; Xie et al., 2018), blueberries (Tan et al., 2018), pomegranate fruits (Munera et al., 2019), and eggplant fruits (Tsouvaltzis et al., 2020). Furthermore, other colour spaces were designed for pomegranate fruits (Fashi et al., 2019) and paprika (Palacios-Morillo et al., 2016). Several types of colour features have been widely used in previous works, such as the mean and standard deviation (Fashi et al., 2019; Mim et al., 2018; Septiarini et al., 2019) and the discretization of histograms (Taparugssanagorn et al., 2015; Zhang et al., 2014). However, in several cases, to achieve high optical performance, the maturity classification of colour features was combined with texture, shape, or both features. Texture features such as contrast, entropy, variance, homogeneity, and skewness were used to classify pomegranate and date fruits (Fashi et al., 2019; Zhang et al., 2014). Moreover, shape features, including area, perimeter, euler, convex area, solidity, and thickness, as well as minor and major arc lengths, were applied to classify apricots (Yang et al., 2019).

Feature extraction generally produces a large number of features. Some of these features are not of value and so have to be discarded through the process of feature selection. PCA is a popular feature selection method and has been widely used in various cases (Fadilah et al., 2012; Munera et al., 2019; Zhang et al., 2014). Other feature selection methods include the correlation-based attribute evaluator, best first search (Mim et al., 2018), and the forward feature selection algorithm (Li et al., 2014).

In classification, several methods can produce optimal performance. K-nearest neighbour (KNN) is the simplest method and has been implemented to detect the maturity of oil palm fruit based on the RGB and HSI colour spaces (Makky and Soni, 2013). In another case, histogram-oriented gradient (HOG) feature vectors based on the $L^*a^*b^*$ colour space were used for blueberry maturity detection. At present, learning methods such as support vector machines (SVMs), ANNs, and

convolutional neural networks (CNNs) have been widely implemented. An SVM with features generated based on a RGB colour space was applied to detect defective apples (Tan et al., 2018), perform the cultivar classification of apricots (Yang et al., 2019), and grade oil palm fruits (Septiarini et al., 2019).

Furthermore, ANNs have been used to classify various fruits, such as oil palm fruit in the HSI colour space (Shabdin et al., 2016), bananas by converting the RGB colour space into HSV and $L^*a^*b^*$ colour spaces (Sanaeifar et al., 2016), and pomegranates using fifteen features produced from the colour spaces of RGB, HSV, YCbCr, and YIQ (Fashi et al., 2019). Subsequently, a CNN was applied to determine kinds of fruits and vegetables (Le et al., 2019; Steinbrener et al., 2019). Several other methods have been applied for fruit classification, such as the random forest for banana classification based on colour features using RGB colour values and shape features using the length of the top middle finger of the banana tier (Piedad et al., 2018), linear discriminant analysis for grading the maturity of oil palm fresh fruit bunches in the RGB colour space (Ali et al., 2020), and clustering to identify blueberries on the red (R), blue (B) and hue (H) channels selected using a forward feature selection algorithm (Li et al., 2014).

In particular, this work proposed a maturity classification method of FFB based on a machine vision approach using mean and entropy features in the YIQ and YCbCr colour spaces combined with back-propagation as the classifier. This method aimed to determine the maturity level of the FFB based on the input image. The maturity level was divided into three classes: raw, ripe, and half-ripe.

2. Materials and methods

2.1. Oil palm fresh fruit bunch samples

The dataset used in this work was a set of images of oil palm FFB acquired from an oil palm plantation in Paser District, East Kalimantan, Indonesia. The images were captured using a built-in digital camera on a smartphone (Samsung A50) and collected in JPEG format measuring 4032×3024 pixels. The acquisition process was carried out in an outdoor area with sufficient bright lighting within an approximate distance of ± 10 cm between the FFB and the camera. The dataset consisted of three classes of FFB maturity levels: raw, ripe, and half-ripe. A total of 240 FFB images were collected with 80 images for each class. The images were then randomly divided into two sets: a training set and a testing set. Both of the sets consisted of 120 images (40 raw, 40 ripe, and 40 half-ripe). Examples of FFB images with different maturity levels are presented in Fig. 1.

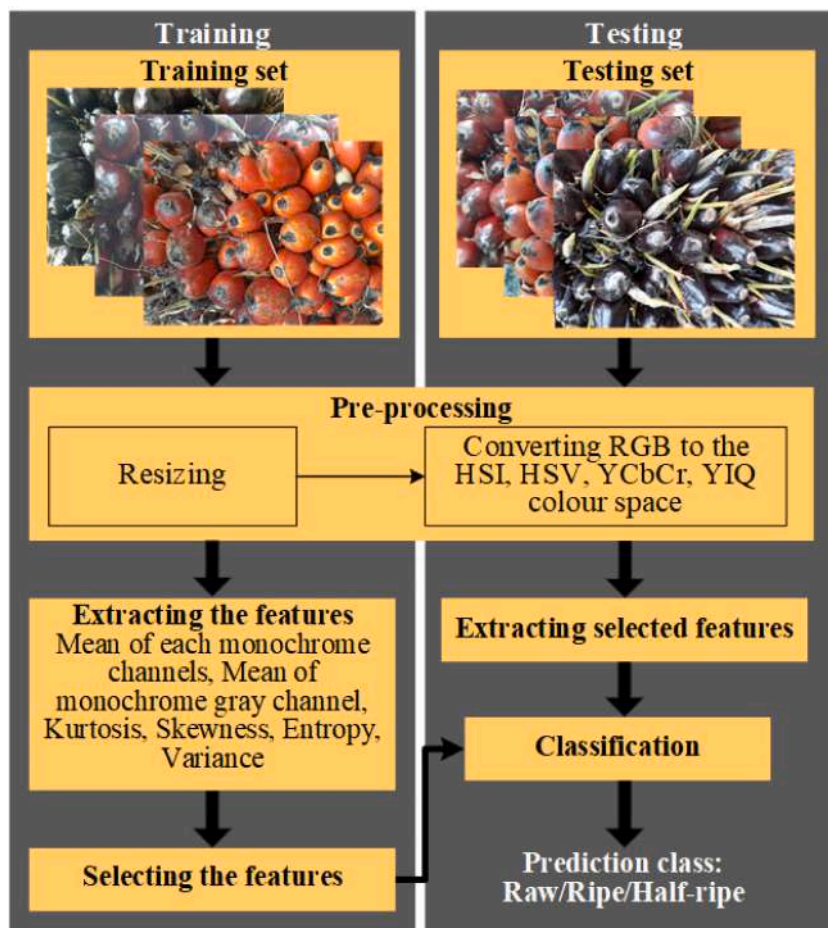


Fig. 2. Overview of all processes in the proposed method of maturity classification.

2.2. Proposed method of maturity classification

The proposed method aimed to predict the maturity class of all FFB images in the testing set. It was divided into two stages, namely, training and testing, where the input for each stage was acquired from the training set and testing set. Both of the stages had two main processes: (1) pre-processing and (2) feature extraction. However, each stage was implemented differently. In the training stage, pre-processing was applied by converting the RGB colour space into HSI, HSV, YCbCr, and YIQ colour spaces. Afterwards, feature extraction was performed on the five colour spaces. Subsequently, the process of feature selection was implemented to select the most important features and to simplify the classification process in the testing stage. In the testing stage, pre-processing only converted RGB to the selected colour space from the feature selection. In the proposed method, the selected features were generated based on the colour spaces of YIQ and YCbCr. Furthermore, the selected extracted feature was applied by referring to the result of feature selection. In the last stage, classification was performed to obtain a prediction class (raw/ripe/half-ripe) from an input of selected features. An overview of all processes in the training and testing stages is depicted in Fig. 2.

2.2.1. Pre-processing

The appropriate pre-processing scheme reduces the computation time. In previous works, the optimization of the computation time was overcome by decreasing the image resolution and reforming the original images to square images (Darwish et al., 2020; Le et al., 2019; Zhang et al., 2014). This work formed a square subimage by resizing the original image from 4032 × 3024 pixels to 640 × 640 pixels (Le et al.,

2019). In pre-processing, it is necessary to convert the colour space to an appropriate colour space in order to optimize the classification results. RGB is a general colour space used in work related to the maturity classification of fruit. Nevertheless, previous works used other colour spaces, such as HSI, HSV, YCbCr, and YIQ. The use of these colour spaces requires a conversion process based on the values in the RGB colour space, which are defined as follows (Garcia-Lamont et al., 2018):

HSI colour space

Converting RGB to the HSI colour space produced elements of hue (H), saturation (S), and intensity (I). Those values were computed using Eqs. (1)- (4).

$$H = \begin{cases} \theta, & B \leq G \\ 360 - \theta, & B > G \end{cases} \tag{1}$$

where

$$\theta = \cos^{-1} \left\{ \frac{\frac{1}{2}[(R - G) + (R - B)]}{[x(R - G)^2 + (R - B)(G - B)]^{1/2}} \right\} \tag{2}$$

$$S = 1 - \frac{[\min(R, G, B)]}{I} \tag{3}$$

$$I = \frac{1}{3}(R + G + B) \tag{4}$$

HSV colour space

Converting RGB to the HSV colour space generated the hue (H) elements calculated by Eq. (1)-(2), saturation (S), and value (V). The values of S and V were computed using Eqs. (5) - (6).

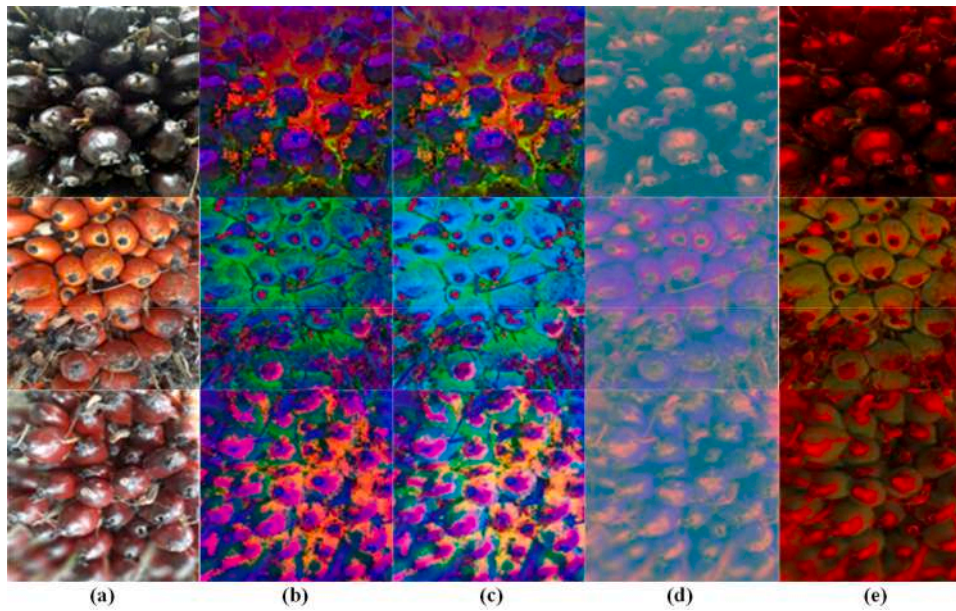


Fig. 3. The resulting images of pre-processing in different colour spaces: (a) RGB, (b) HSI, (c) HSV, (d) YCbCr, and (e) YIQ.

$$S = \begin{cases} 0, & \max(R, G, B) = 0 \\ 1 - \frac{\min(R, G, B)}{\max(R, G, B)}, & \text{otherwise} \end{cases} \quad (5)$$

$$V = \max(R, G, B) \quad (6)$$

YCbCr colour space

Converting from RGB to the YCbCr colour space produced three elements: luminance (Y), the blue-difference component (Cb) and the red-difference component (Cr). The value of each element in the colour space was calculated using Eq. (7).

$$\begin{bmatrix} Y \\ Cb \\ Cr \end{bmatrix} = \begin{bmatrix} 16 \\ 128 \\ 128 \end{bmatrix} + \begin{bmatrix} 65.481 & 128.553 & 24.966 \\ -37.797 & -74.203 & 112.00 \\ 112.00 & -93.786 & -18.214 \end{bmatrix} \begin{bmatrix} R \\ G \\ B \end{bmatrix} \quad (7)$$

YIQ colour space

Converting from RGB to the YIQ colour space resulted in three components: the luminance (Y) and I and Q, both of which represent the chromatic components. The values of the YIQ colour space elements were calculated using Eq. (8).

$$\begin{bmatrix} Y \\ I \\ Q \end{bmatrix} = \begin{bmatrix} 0.299 & 0.587 & 0.114 \\ 0.596 & -0.274 & -0.322 \\ 0.211 & -0.523 & 0.312 \end{bmatrix} \begin{bmatrix} R \\ G \\ B \end{bmatrix} \quad (8)$$

Fig. 3 shows several examples of the pre-processing results for images with a maturity levels of raw, ripe, and half-ripe. The resizing of the form to a square image is depicted in Fig. 3. Column (a) in Fig. 3 shows the results in the RGB colour space, followed by the HSI, HSV, YCbCr, and YIQ colour spaces depicted by columns (b), (c), (d), and (e), respectively.

2.2.2. Feature extraction

Feature extraction was carried out based on colour and texture because both features have been used successfully in previous works related to the classification of fruit and other objects (Duysak and Yigit, 2020; Fashi et al., 2019; Mim et al., 2018; Y. Zhang et al., 2014). This process was applied to five colour spaces: RGB, HSI, HSV, YCbCr, and YIQ. A total of 40 features were extracted in this work. Those features were (1) the mean (μ) of each monochrome channel in the five colour spaces: the mean value of the R channel (μ_R), the mean value of the G channel (μ_G), and the mean value of the B channel (μ_B) for the RGB

colour space; the mean value of the H channel (μ_H), the mean value of the S channel (μ_{S1}), and the mean value of the I channel (μ_I) for the HSI colour space; the mean value of the H channel (μ_H), the mean value of the S channel (μ_{S2}), and the mean value of the V channel (μ_V) for the HSV colour space; the mean value of the Y channel (μ_Y), the mean value of the Cb channel (μ_{Cb}), and the mean value of the Cr channel (μ_{Cr}) for the YCbCr colour space; and the mean value of the Y channel (μ_Y), the mean value of the I channel (μ_{I2}), and the mean value of the Q channel (μ_Q) for the YIQ colour space. This feature is defined in Eq. (9):

$$\mu_x = \frac{1}{MN} \sum_{i=1}^M \sum_{j=1}^N p_{ij} \quad (9)$$

where X is the monochrome channel, M and N are the image dimensions, and p_{ij} is the value of the monochrome channel in row j and column i.

The aforementioned features were used to calculate (2) the mean of the monochrome grey channel in the RGB (μ_{RGB}), HSI (μ_{HSI}), HSV (μ_{HSV}), YCbCr (μ_{YCbCr}), and YIQ (μ_{YIQ}) colour spaces. These features were generated by replacing the value of p_{ij} in Eq. (9) with the value of the monochrome grey channel. Subsequently, (3) the variance (σ^2) values in the RGB (σ^2_{RGB}), HSI (σ^2_{HSI}), HSV (σ^2_{HSV}), YCbCr (σ^2_{YCbCr}), and YIQ (σ^2_{YIQ}) colour spaces, (4) the kurtosis (γ) values in the RGB (γ_{RGB}), HSI (γ_{HSI}), HSV (γ_{HSV}), YCbCr (γ_{YCbCr}), and YIQ (γ_{YIQ}) colour spaces, (5) the skewness (θ) values in the RGB (θ_{RGB}), HSI (θ_{HSI}), HSV (θ_{HSV}), YCbCr (θ_{YCbCr}), and YIQ (θ_{YIQ}) colour spaces, and (6) the entropy (H_n) values in the RGB (H_{RGB}), HSI (H_{HSI}), HSV (H_{HSV}), YCbCr (H_{YCbCr}), and YIQ (H_{YIQ}) colour spaces were also computed. These features are defined in Eqs. (10)-(13) (Attique et al., 2018; Turkoglu and Hanbay, 2019):

$$\sigma^2 = \frac{\sum_{i=1}^M \sum_{j=1}^N (p_{ij} - \mu)^2}{MN - 1} \quad (10)$$




$$\gamma = \frac{\sum_{i=1}^M \sum_{j=1}^N (p_{ij} - \mu)^4}{MN\sigma^4} - 3 \quad (11)$$

$$\theta = \frac{\sum_{i=1}^M \sum_{j=1}^N (p_{ij} - \mu)^3}{MN\sigma^3} \quad (12)$$

$$H_n = \sum_{i=1}^M \sum_{j=1}^N p(i,j) \log_2 p(i,j) \quad (13)$$

Table 1

The results of implementing the extracted features with three different feature selection methods

ROI image	Features selection method		
	PCA	CFS	Gain ratio
	$H_{YIQ} = 5.35$	$\mu_{YCbCr} = 121.04$	$H_{YCbCr} = 6.18$
	$\mu_{Cr} = 129.14$	$H_{YCbCr} = 6.18$	$\mu_S = 0.41$
	$H_{YCbCr} = 6.18$		$\mu_{Cb} = 126.94$
	$\mu_{I2} = 0.01$		$\mu_{I2} = 0.01$
	$\mu_{YIQ} = 37.12$		$\mu_{Cr} = 129.14$
			$\gamma_{YCbCr} = 1.88$
	$H_{YIQ} = 6.69$	$\mu_{YCbCr} = 125.27$	$H_{YCbCr} = 7.06$
	$\mu_{Cr} = 147.75$	$H_{YCbCr} = 7.06$	$\mu_S = 0.41$
	$H_{YCbCr} = 7.06$		$\mu_{Cb} = 114.55$
	$\mu_{I2} = 0.12$		$\mu_{I2} = 0.12$
	$\mu_{YIQ} = 49.86$		$\mu_{Cr} = 147.75$
			$\gamma_{YCbCr} = 0.43$
	$H_{YIQ} = 6.18$	$\mu_{YCbCr} = 126.99$	$H_{YCbCr} = 6.80$
	$\mu_{Cr} = 141.72$	$H_{YCbCr} = 6.80$	$\mu_S = 0.32$
	$H_{YCbCr} = 6.80$		$\mu_{Cb} = 122.67$
	$\mu_{I2} = 0.07$		$\mu_{I2} = 0.07$
	$\mu_{YIQ} = 48.11$		$\mu_{Cr} = 141.72$
			$\gamma_{YCbCr} = 1.25$

2.2.3. Feature selection

In this work, a total of 40 features were extracted. This required time-consuming computations and led to a complicated classification process. Therefore, feature selection was needed to obtain dominant features with an important role in the classification. Such features were only extracted in selected colour spaces. Three feature selection methods—principal component analysis (PCA), correlation feature selection (CFS), and the gain ratio—were performed due to their ability to successfully and significantly reduce the number of features while producing optimal classification results in previous works. Moreover, these methods have been applied to various types of objects related to this work (Fadilah et al., 2012; Zhang et al., 2014; Munera et al., 2019). These studies used Weka 3.8 to obtain the selected features. The results of the PCA, CFS, and gain ratio methods consisted of five features (H_{YIQ} , μ_{Cr} , H_{YCbCr} , μ_{I2} , μ_{YIQ}), two features (μ_{YCbCr} , H_{YCbCr}), and six features (H_{YCbCr} , μ_S , μ_{Cb} , μ_{I2} , μ_{Cr} , γ_{YCbCr}), respectively. Examples of the selected features of images with different maturity levels are presented in Table 1.

2.2.4. Classification

The selected features were generated by applying the PCA, CFS, and gain ratio methods and subsequently used as inputs in the classification process. To justify the proposed methods, three popular classifiers—naïve Bayes, SVM, and ANN—were used to obtain the optimal results. These methods have been widely implemented because they have successfully classified various types of fruit objects (Yang et al., 2019; Piedad et al., 2018; Tu et al., 2018). In this work, an ANN was implemented because it obtained the optimal classification results with five features using PCA (H_{YIQ} , μ_{Cr} , H_{YCbCr} , μ_{I2} , μ_{YIQ}). An ANN is a supervised method that is generally applied in the classification process. A feedback neural network with a back-propagation training algorithm was implemented. This network operates by adapting biological neurons with a structure consisting of three layers: an input layer, hidden layers, and an output layer. The number of hidden layers is one or more, and the justification of the number of layers does not have certain rules; the number is determined based on empirical experiments (Yang et al.,

		Prediction class		
		A_1	A_2	A_3
Actual class	A_1	N_{11}	N_{12}	N_{13}
	A_2	N_{21}	N_{22}	N_{23}
	A_3	N_{31}	N_{32}	N_{33}

N_{ij}

Fig. 4. Confusion matrix for multiple classes classification

2019; Nturambirwe and Opara, 2020). The input layer consisted of five neurons according to the number of features, while the output layer included three neurons. Moreover, the number of hidden layers (l) was obtained based on the number of neurons in the output layer (m) and the number of neurons in the input layer (n), and a constant value (a) between 0 and 10. Thus, the number of hidden layers was computed using Eq. (14) (Yang et al., 2019):

$$l < (m + n) + a \tag{14}$$

There were three values of parameters needed to build the ANN structure, namely, the maximum iteration or epoch, the learning rate, and the error rate; the values used in this work were 100, 0.1, and 0.0004, respectively (Yang, 2019). To evaluate the proposed method, a training dataset consisting of 120 images (40 raw, 40 ripe, and 40 half-ripe) was used at this stage.

3. Result

3.1. Performance measures

The performance of the proposed method was evaluated based on the confusion matrix that presents the information regarding the predicted class of oil palm fruit maturity as a result of the proposed method against the actual class. The maturity level of oil palm fruit was divided into three classes: raw (A_1), ripe (A_2), and half-ripe (A_3). The confusion matrix for the multiple classes in this work is depicted in Fig. 4. In this matrix, N_{ij} denotes the number of images that should be classified as class A_i but are instead classified as class A_j by the proposed method.

In this work, three parameters were employed to represent the performance of the proposed method: precision, recall, and accuracy. Each of these values were between 0 and 1. The proposed method was declared robust and successful if the value was close to 1. The performance measures were computed using Eqs. (15)–(17) with n as the number of images in the testing dataset (Deng et al., 2016):

$$Precision = \frac{N_{ii}}{\sum_{k=1}^n N_{ki}} \tag{15}$$

$$Recall = \frac{N_{ii}}{\sum_{k=1}^n N_{ik}} \tag{16}$$

Table 2

The results of implementing various feature extraction and classification methods

Classifier	Features selection	Performance measures		
		Prec (%)	Rec (%)	Acc (%)
Naïve Bayes	PCA	98.3	96.7	96.7
	CFS	93.2	92.5	92.5
	Gain ratio	96.2	95.8	95.8
SVM	PCA	97.6	97.5	97.5
	CFS	93.5	93.3	93.3
	Gain ratio	96.2	95.8	95.8
ANN	PCA	98.4	98.3	98.3
	CFS	96.2	95.8	95.8
	Gain ratio	98.4	98.3	98.3

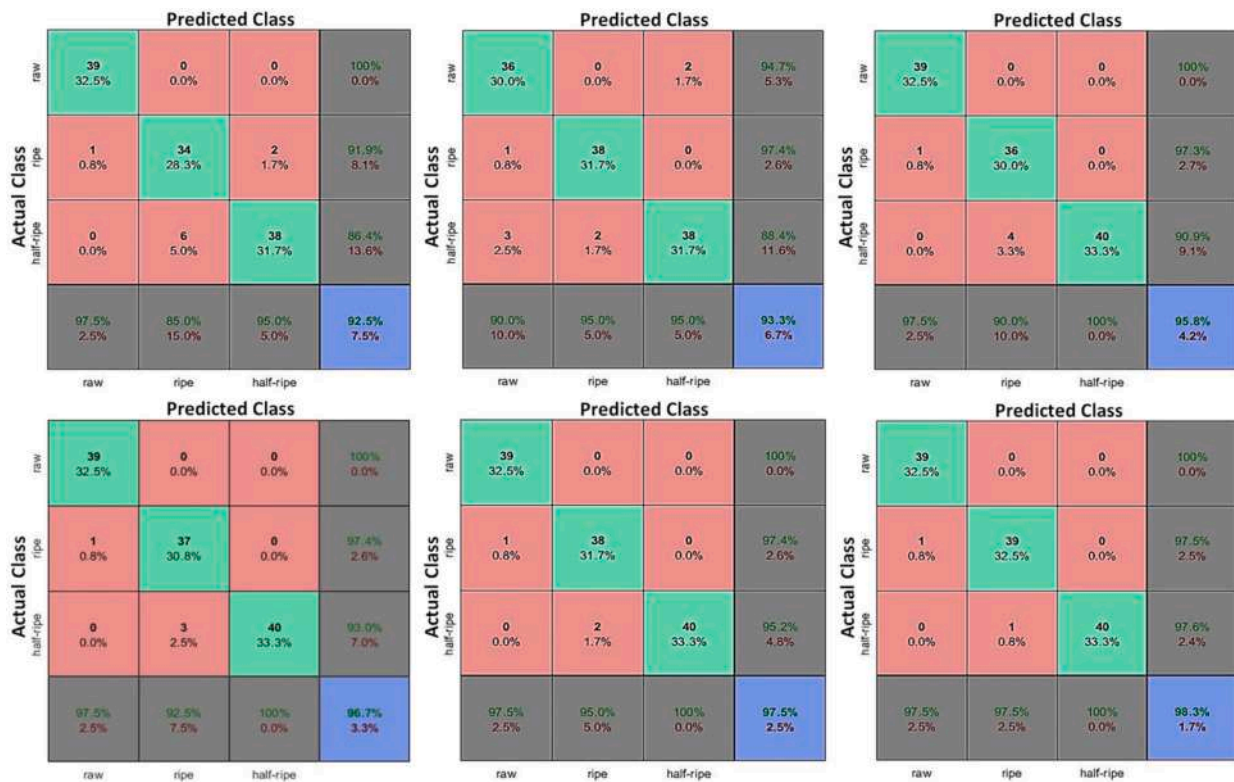


Fig. 5. Confusion matrix of classification results (raw, ripe, and half-ripe)

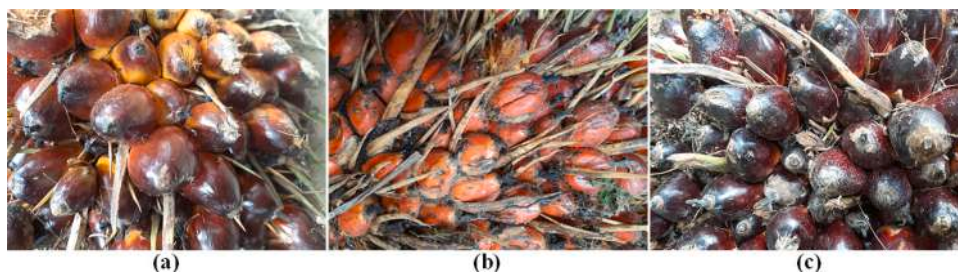


Fig. 6. Misclassification examples of images: (a) half-ripe classified as raw, (b) half-ripe classified as raw, and (c) half-ripe classified as raw

$$Accuracy = \frac{\sum_{i=1}^n N_{ii}}{\sum_{i=1}^n \sum_{j=1}^n N_{ij}} \quad (17)$$

3.2. Performance evaluation

The performance evaluation of the proposed method was carried out by applying different feature selection and classification methods to justify the most appropriate and robust method against the dataset used. In this work, a testing dataset consisting of 120 images (40 raw, 40 ripe, and 40 half-ripe) was used to perform the evaluation. The performance evaluation results obtained by implementing the various methods of feature selection and classification based on three parameters, namely, precision (*Prec*), recall (*Rec*), and accuracy (*Acc*), are summarized in Table 2.

Table 2 shows that for all of the evaluation results, an accuracy of 90% was achieved by successfully using various methods of feature selection and classification. The highest accuracy was 98.3%, which was obtained using the PCA and ANN methods as well as the gain ratio and ANN. Therefore, the proposed method implemented the PCA and ANN methods because PCA only produced five features (H_{YIQ} , μ_{Cr} , H_{YCbCr} , μ_{I2} , μ_{YQ}), while the gain ratio generated six features (H_{YCbCr} , μ_S , μ_{Cb} , μ_{I2} , μ_{Cr} ,

γ_{YCbCr}).

To present the details of the comprehensive analysis, several examples of the confusion matrix that correspond to the results of the performance evaluation (Table 2) are depicted in Fig. 5. There were three types of misclassifications of maturity levels that occurred. First, the half-ripe FFB in the actual class was classified as ripe in the predicted class; this error occurred most frequently. This misclassification was caused because the colours of the half-ripe and ripe FFB visually appear more similar to each other than do the half-ripe and raw FFB and the ripe and raw FFB. Moreover, the occurrence of uneven colour changes is shown in Fig. 6 (a). The feature values of the FFB tend to be closer between half-ripe and ripe fruits, as shown in Table 1. Second, ripe FFB in the actual class was classified as raw in the predicted class. This misclassification occurred only once for each classification result. It occurred against the ripe image where the fruit area was covered by noise such as sand or dark soil, which consequently made the colour of the FFB resemble the level of raw maturity, as shown in Fig. 6 (b).

4. Discussion

Determining the maturity level of oil palm fruit plays an important role in the harvesting process because it affects the amount of oil

produced. The palm oil produced will be optimal if the fruit is harvested at the appropriate maturity level. If oil palm fruit is harvested at half-ripe or overripe levels, the amount of oil produced will be lower. This work developed a classification method for the maturity level by combining the PCA (which generated five features) and ANN methods. The proposed method can distinguish three levels of maturity (raw, ripe, and half-ripe) in accordance with the objectives of this work and indicates favourable performance, achieving a 98.3% accuracy.

The performance of the proposed method showed that this technique can compete with the methods developed in previous works. In previous works related to the maturity classification of FFB, an ANN was applied (Fadilah et al., 2012) using the features extracted from the hue channel and successfully achieved an accuracy of 93.33%. In addition, using the features produced based on the HIS colour space achieved an accuracy of 70% (Shabdin et al., 2016). In contrast, two colour spaces (RGB and HSI) were used to obtain texture features by applying the squared Euclidean distance in the classification process, achieving an accuracy of 93.53% (Makky and Soni, 2013). Partial least squares and PCA methods were applied with the features from the RGB colour space to determine the maturity level consisting of three classes, namely, unripe, ripe, and overripe, using linear discriminant analysis and a quadratic discriminant as a classifier that succeeded in achieving an accuracy exceeding 85% (Ali et al., 2020). Furthermore, an inductive sensor system aimed to identify FFB maturity on smartphones was developed and achieved an accuracy of 100%; nevertheless, the system only distinguished two classes, namely, ripe or unripe (Sinambela et al., 2020).

5. Conclusion

This work proposed a maturity classification method of oil palm FFB using colour and texture features. Forty features were extracted from several colour spaces, which were reduced to five features (H_{YIQ} , μ_{Cr} , H_{YCbCr} , μ_{I2} , μ_{YIQ}) using the PCA method to optimize the computation time. Furthermore, the classification was applied using an ANN to distinguish three classes: raw, ripe, and half-ripe. The proposed method was evaluated using a local testing dataset of 120 images consisting of those classes. Measurements of precision, recall, and accuracy indicated that the proposed method successfully achieved values of 98.4%, 98.3%, and 98.3%, respectively. The misclassification of half-ripe FFB as ripe FFB occurred due to uneven fruit colour changes. The limitation of this work will be enhanced by improving the image acquisition technique and discarding detailed noise covering the fruit area. Moreover, the classification method is still widely open to further development to distinguish FFB into more than three classes.

Credit Author Statement

Author	Contributions
Anindita Septiarini	Conceptualization, Methodology, Validation, Formal analysis, Writing - Original Draft, Supervision, Funding acquisition
Hamdani Hamdani	Methodology, Software, Data Curation, Project administration
Heliza Rahmania Hatta	Software, Investigation, Resources
Anita Ahamd Kasim Fitri Utamingrum	Writing - Review & Editing, Visualization Methodology, Validation, Formal analysis

Declaration of Competing Interest

None

Acknowledgement

This work was funded by RISTEK-BRIN Indonesia in 2020 [Grant No. 213/UN17.41/AMD/KL/2020].

References

- Aji, A.F., Munajat, Q., Pratama, A.P., Kalamullah, H., Aprinaldi Setiawan, J., Arymurthy, A.M., 2013. Detection of Palm Oil Leaf Disease with Image Processing and Neural Network Classification on Mobile Device. *Int. J. Comput. Theory Eng.* 5, 528–532. <https://doi.org/10.7763/ijctc.2013.v5.743>.
- Ali, M.M., Hashim, N., Hamid, A.S.A., 2020. Combination of laser-light backscattering imaging and computer vision for rapid determination of oil palm fresh fruit bunches maturity. *Comput. Electron. Agric.* 169, 105235 <https://doi.org/10.1016/j.compag.2020.105235>.
- Darwish, A., Ezzat, D., Hassanien, A.E., 2020. An optimized model based on convolutional neural networks and orthogonal learning particle swarm optimization algorithm for plant diseases diagnosis. *Swarm Evol. Comput.* 52, 100616 <https://doi.org/10.1016/j.swevo.2019.100616>.
- Deng, X., Liu, Q., Deng, Y., Mahadevan, S., 2016. An improved method to construct basic probability assignment based on the confusion matrix for classification problem. *Information Sci.* 340–341, 250–261. <https://doi.org/10.1016/j.ins.2016.01.033>.
- Fadilah, N., Mohamad-Saleh, J., Halim, Z.A., Ibrahim, H., Ali, S.S.S., 2012. Intelligent color vision system for ripeness classification of oil palm fresh fruit bunch. *Sensors* 12, 14179–14195. <https://doi.org/10.3390/s121014179>.
- Fahmi, F., Trianda, D., Andayani, U., Siregar, B., 2018. Image processing analysis of geospatial uav orthophotos for palm oil plantation monitoring. *J. Phys. Conf. Ser.* 978, 0–7. <https://doi.org/10.1088/1742-6596/978/1/012064>.
- Fashi, M., Naderloo, L., Javadikia, H., 2019. The relationship between the appearance of pomegranate fruit and color and size of arils based on image processing. *Postharvest Biol. Technol.* 154, 52–57. <https://doi.org/10.1016/j.postharvbio.2019.04.017>.
- Garcia-Lamont, F., Cervantes, J., López, A., Rodriguez, L., 2018. Segmentation of images by color features: A survey. *Neurocomputing* 292, 1–27. <https://doi.org/10.1016/j.neucom.2018.01.091>.
- Hafiz, M., Hazir, M., Rashid, A., Shariff, M., Din, M., Rahman, A., Saripan, M.I., 2012. Oil palm bunch ripeness classification using fluorescence technique. *J. Food Eng.* 113, 534–540. <https://doi.org/10.1016/j.jfoodeng.2012.07.008>.
- Hamdani, Septiarini, A., Khairina, D.M., 2016. Model Assessment of Land Suitability Decision Making for Oil Palm Plantation. In: *Proceeding - 2016 International Conference on Science in Information Technology (ICSITech) 2016*. <https://doi.org/10.1109/ICSITech.2016.7852617>, pp. 109–113. <https://doi.org/10.1109/ICSITech.2016.7852617>.
- Hameed, K., Chai, D., Rassau, A., 2018. A comprehensive review of fruit and vegetable classification techniques. *Image Vis. Comput.* 80, 24–44. <https://doi.org/10.1016/j.imavis.2018.09.016>.
- Jana, S., Parekh, R., Sarkar, B., 2020. A De novo approach for automatic volume and mass estimation of fruits and vegetables. *Optik (Stuttg.)* 200, 163443. <https://doi.org/10.1016/j.jileo.2019.163443>.
- Ji, Y., Sun, L., Li, Y., Li, J., Liu, S., Xie, X., Xu, Y., 2019. Non-destructive classification of defective potatoes based on hyperspectral imaging and support vector machine. *Infrared Phys. Technol.* 99, 71–79. <https://doi.org/10.1016/j.infrared.2019.04.007>.
- Khaled, A.Y., Abd Aziz, S., Bejo, S.K., Nawi, N.M., Seman, I.A., 2018. Spectral features selection and classification of oil palm leaves infected by Basal stem rot (BSR) disease using dielectric spectroscopy. *Comput. Electron. Agric.* 144, 297–309. <https://doi.org/10.1016/j.compag.2017.11.012>.
- Le, T.T., Lin, C.Y., Piedad, E.J., 2019. Deep learning for noninvasive classification of clustered horticultural crops – A case for banana fruit tiers. *Postharvest Biol. Technol.* 156, 110922 <https://doi.org/10.1016/j.postharvbio.2019.05.023>.
- Li, H., Lee, W.S., Wang, K., 2014. Identifying blueberry fruit of different growth stages using natural outdoor color images. *Comput. Electron. Agric.* 106, 91–101. <https://doi.org/10.1016/j.compag.2014.05.015>.
- Makky, M., Soni, P., 2013. Development of an automatic grading machine for oil palm fresh fruit bunches (FFBs) based on machine vision. *Comput. Electron. Agric.* 93, 129–139. <https://doi.org/10.1016/j.compag.2013.02.008>.
- Mim, F.S., Galib, S.M., Hasan, M.F., Jerin, S.A., 2018. Automatic detection of mango ripening stages – An application of information technology to botany. *Sci. Hortic. (Amsterdam)* 237, 156–163. <https://doi.org/10.1016/j.scienta.2018.03.057>.
- Mohammed, O., Saeed, B., Sankaran, S., Rashid, A., Shariff, M., Zulhaidi, H., Shafri, M., Ehsani, R., Salem, M., Hafiz, M., Hazir, M., 2012. Classification of oil palm fresh fruit bunches based on their maturity using portable four-band sensor system. *Comput. Electron. Agric.* 82, 55–60. <https://doi.org/10.1016/j.compag.2011.12.010>.
- Munera, S., Hernández, F., Aleixos, N., Cubero, S., Blasco, J., 2019. Maturity monitoring of intact fruit and arils of pomegranate cv. ‘Mollar de Elche’ using machine vision and chemometrics. *Postharvest Biol. Technol.* 156, 110936 <https://doi.org/10.1016/j.postharvbio.2019.110936>.
- Nturambirwe, J.F.I., Opara, U.L., 2020. Machine learning applications to non-destructive defect detection in horticultural products. *Biosyst. Eng.* 189, 60–83. <https://doi.org/10.1016/j.biosystemseng.2019.11.011>.
- Palacios-Morillo, A., Jurado, J.M., Alcázar, A., Pablos, F., 2016. Differentiation of Spanish paprika from Protected Designation of Origin based on color measurements and pattern recognition. *Food Control* 62, 243–249. <https://doi.org/10.1016/j.foodcont.2015.10.045>.
- Pamornnak, B., Limsiroratanana, S., Khaorapong, T., 2017. An automatic and rapid system for grading palm bunch using a Kinect camera. *Comput. Electron. Agric.* 143, 227–237. <https://doi.org/10.1016/j.compag.2017.10.020>.
- Pérez-Zavala, R., Torres-Torriti, M., Cheein, F.A., Troni, G., 2018. A pattern recognition strategy for visual grape bunch detection in vineyards. *Comput. Electron. Agric.* 151, 136–149. <https://doi.org/10.1016/j.compag.2018.05.019>.
- Piedad, E., Larada, J.I., Pojas, G.J., Ferrer, L.V.V., 2018. Postharvest classification of banana (*Musa acuminata*) using tier-based machine learning. *Postharvest Biol. Technol.* 145, 93–100. <https://doi.org/10.1016/j.postharvbio.2018.06.004>.

- Sanaeifar, A., Bakhsipour, A., de la Guardia, M., 2016. Prediction of banana quality indices from color features using support vector regression. *Talanta* 148, 54–61. <https://doi.org/10.1016/j.talanta.2015.10.073>.
- Septiariini, A., Hamdani, H., Hatta, H.R., Anwar, K., 2020. Automatic image segmentation of oil palm fruits by applying the contour-based approach. *Sci. Hortic. (Amsterdam)*. 261, 108939 <https://doi.org/10.1016/j.scienta.2019.108939>.
- Septiariini, A., Hamdani, H., Hatta, H.R., Kasim, A.A., 2019. Image-based processing for ripeness classification of oil palm fruit. In: *Proceeding - 2019 5th Int. Conf. Sci. Inf. Technol. Embrac. Ind. 4.0 Towar. Innov. Cyber Phys. Syst. ICSITech 2019*, pp. 23–26. <https://doi.org/10.1109/ICSITech46713.2019.8987575>.
- Shabdin, M.K., Shariff, A.R.M., Johari, M.N.A., Saat, N.K., Abbas, Z., 2016. A study on the oil palm fresh fruit bunch (FFB) ripeness detection by using Hue, Saturation and Intensity (HSI) approach. *IOP Conf. Ser. Earth Environ. Sci.* 37 <https://doi.org/10.1088/1755-1315/37/1/012039>.
- Shiddiq, M., Anjasmara, R., Sari, N., 2017. Ripeness Detection Simulation of Oil Palm Fruit Bunches Using Laser-Based Imaging System. In: *AIP Conference Proceedings. American Institute of Physics*. <https://doi.org/10.1063/1.4973101>.
- Sinambela, R., Mandang, T., Subrata, I.D.M., Hermawan, W., 2020. Application of an inductive sensor system for identifying ripeness and forecasting harvest time of oil palm. *Sci. Hortic. (Amsterdam)*. 265, 109231 <https://doi.org/10.1016/j.scienta.2020.109231>.
- Steinbrener, J., Posch, K., Leitner, R., 2019. Hyperspectral fruit and vegetable classification using convolutional neural networks. *Comput. Electron. Agric.* 162, 364–372. <https://doi.org/10.1016/j.compag.2019.04.019>.
- Tan, K., Lee, W.S., Gan, H., Wang, S., 2018. Recognising blueberry fruit of different maturity using histogram oriented gradients and colour features in outdoor scenes. *Biosyst. Eng.* 176, 59–72. <https://doi.org/10.1016/j.biosystemseng.2018.08.011>.
- Tan, W., Sun, L., Yang, F., Che, W., Ye, D., Zhang, D., Zou, B., 2018. Study on bruising degree classification of apples using hyperspectral imaging and GS-SVM. *Optik (Stuttg)* 154, 581–592. <https://doi.org/10.1016/j.ijleo.2017.10.090>.
- Taparugssanagorn, A., Siwamogsatham, S., Pomalaza-ráez, C., 2015. A non-destructive oil palm ripeness recognition system using relative entropy. *Comput. Electron. Agric.* 118, 340–349. <https://doi.org/10.1016/j.compag.2015.09.018>.
- Tsouvaltzi, P., Babellahi, F., Amodio, M.L., Colelli, G., 2020. Early detection of eggplant fruit stored at chilling temperature using different non-destructive optical techniques and supervised classification algorithms. *Postharvest Biol. Technol.* 159, 111001 <https://doi.org/10.1016/j.postharvbio.2019.111001>.
- Tu, S., Xue, Y., Zheng, C., Qi, Y., Wan, H., Mao, L., 2018. Detection of passion fruits and maturity classification using Red-Green-Blue Depth images. *Biosyst. Eng.* 175, 156–167. <https://doi.org/10.1016/j.biosystemseng.2018.09.004>.
- Xie, C., Chu, B., He, Y., 2018. Prediction of banana color and firmness using a novel wavelengths selection method of hyperspectral imaging. *Food Chem* 245, 132–140. <https://doi.org/10.1016/j.foodchem.2017.10.079>.
- Yang, X., Zhang, R., Zhai, Z., Pang, Y., Jin, Z., 2019. Machine learning for cultivar classification of apricots (*Prunus armeniaca* L.) based on shape features. *Sci. Hortic. (Amsterdam)*. 256, 108524 <https://doi.org/10.1016/j.scienta.2019.05.051>.
- Zhang, D., Lee, D.J., Tippetts, B.J., Lillywhite, K.D., 2014. Date maturity and quality evaluation using color distribution analysis and back projection. *J. Food Eng.* 131, 161–169. <https://doi.org/10.1016/j.jfoodeng.2014.02.002>.